

# Comparing Capacity Value Estimation Techniques for Photovoltaic Solar Power

Seyed Hossein Madaeni, *Student Member, IEEE*, Ramteen Sioshansi, *Senior Member, IEEE*, and Paul Denholm, *Senior Member, IEEE*

**Abstract**—We estimate the capacity value of photovoltaic (PV) solar plants in the western U.S. Our results show that PV plants have capacity values ranging between 52% and 93%, depending on location and sun-tracking capability. We further compare more robust but data- and computationally-intense reliability-based estimation techniques to simpler approximation methods. We show that if implemented properly, these techniques provide accurate approximations of reliability-based methods. Overall, methods based on the weighted capacity factor of the plant provide the most accurate estimate. We also examine the sensitivity of PV capacity value to the inclusion of sun-tracking systems.

**Index Terms**—Capacity value, reliability theory, approximation techniques, photovoltaic solar

## NOMENCLATURE

$T$	time index set
$T'$	subset of hours used in capacity factor-based approximation
$\Lambda$	set of locations modeled
$G_t$	conventional generating capacity available in hour $t$
$\bar{G}$	nameplate conventional generating capacity
$V_t$	generating capacity available from photovoltaic (PV) plant in hour $t$
$\mu_{PV}$	mean hourly generating capacity available from PV plant
$\sigma_{PV}$	standard deviation of hourly generating capacity available from PV plant
$\bar{V}$	rated capacity of PV plant
$L_t$	hour- $t$ load
$S_t$	hour- $t$ surplus generation capacity
$\mu_S$	mean of $S_t$
$\sigma_S$	standard deviation of $S_t$
$\bar{L}$	constant loaded added in each hour in effective load-carrying capability (ELCC) calculation

$B_t$	generating capacity available from benchmark unit in hour $t$ in equivalent conventional power (ECP) calculation
$p_t$	hour- $t$ loss of load probability
$\epsilon$	loss of load expectation (LOLE) of base system
$\epsilon^{ELCC}$	LOLE with PV and loads added in ELCC calculation
$\epsilon^{PV}$	LOLE with PV added in ECP calculation
$\epsilon^B$	LOLE with benchmark unit added in ECP calculation
$w_t$	hour- $t$ weight used in capacity factor-based approximation
$m$	system characteristic
$\Omega$	index set for PV plant states in multi-state ELCC approximation
$V_\omega$	PV capacity unavailable in state $\omega$
$\pi_\omega$	probability PV plant is in state $\omega$
$Z$	Z statistic
$c_\lambda^{ELCC}$	average annual ELCC of a PV plant at location $\lambda$
$c_\lambda^a$	average annual capacity value of a PV plant at location $\lambda$ approximated using method $a$

## I. INTRODUCTION

**A**N important issue for power system planners is the contribution of renewables to reliably meeting demand [1], [2]. A generator's ability to help reliably serve load is typically captured by estimating its capacity value [3]–[5]. Generator outages, which can occur due to mechanical failures, planned maintenance, or lack of generating resource in real-time, may leave a power system with insufficient generating capacity to meet load. The issue of real-time resource availability is especially prevalent with renewables. Previous analyses estimate the capacity values of wind [2], [6]–[11], photovoltaic (PV) solar [12]–[16], and concentrating solar power (CSP) [17], [18] resources. They demonstrate that these renewables have non-zero capacity values that can range between 5% and 95% of maximum generating capacity. The range of capacity values reflects the effects of technology, geography, and demand patterns on the coincidence between real-time generation and demand. It also reflects the decreasing marginal capacity value of additional renewables. These analyses use a mix of reliability-based and statistical approximation methods. These methods estimate the probability that a power system experiences an outage event, which is defined as the generating capacity available being less than load. The capacity value is determined based on the contribution of a generator toward reducing this probability.

This paper expands on previous analyses of the capacity value of PV. Using a case study of the western United

This work was supported by the U.S. Department of Energy through prime contract DE-AC36-08GO28308 and by the Alliance for Sustainable Energy, LLC through subcontract AGG-1-11946-01.

S. H. Madaeni was with the Integrated Systems Engineering Department, The Ohio State University, Columbus, OH 43210, USA. He is now with the Short Term Electric Supply Department, Pacific Gas and Electric Company, San Francisco, CA 94105, USA (e-mail: SHM8@pge.com).

R. Sioshansi is with the Integrated Systems Engineering Department, The Ohio State University, Columbus, OH 43210, USA (e-mail: sioshansi.1@osu.edu).

P. Denholm is with the Strategic Energy Analysis Center, National Renewable Energy Laboratory, Golden, CO 80401, USA (e-mail: paul.denholm@nrel.gov).

The opinions expressed and conclusions reached are solely those of the authors and do not represent the official position of Pacific Gas and Electric Company.

States, we estimate that PV has long-run interconnect-wide average capacity values of between 52% and 93% of its rated ac capacity, depending on location, sun-tracking capability, and the reliability-based estimation used. We also examine different approximation techniques, showing that some are quite accurate relative to reliability-based methods. We finally study the sensitivity of the capacity value of PV to the use of single- and double-axis sun-tracking systems. The remainder of this paper is organized as follows: section II summarizes the capacity value estimation techniques that we examine, section III summarizes our case study and the data used, section IV summarizes our results, section V presents our sensitivity analysis, and section VI concludes.

## II. CAPACITY VALUE ESTIMATION TECHNIQUES

### A. Reliability-Based Methods

Numerous techniques are used to approximate the capacity value of conventional and renewable generators. Reliability-based methods are among the most robust and widely accepted of these [1], [5], [7], [9], [10], [17]–[21]. These techniques use a standard power system reliability index, loss of load probability (LOLP), to determine how a generator affects the reliability of the system. LOLP is defined as the probability that generator or transmission outages leave the system with insufficient capacity to serve the load in a given period of time. A related reliability index, loss of load expectation (LOLE), is defined as the sum of LOLPs over some planning horizon, and gives the expected number of outage periods within that horizon. Other reliability metrics, such as loss of energy probability, can also be used. These are less common, however, especially in estimating the capacity value of renewables, and we focus on LOLE-based methods, to make our results directly comparable to these previous works [2], [6]–[18]. LOLPs are typically modeled at hourly timesteps and LOLEs are computed over year-long periods, which are the conventions used in this analysis. Conventional generator and transmission outages are typically modeled using an equivalent forced outage rate (EFOR), which captures the probability of a failure at any given time. With variable renewables, one must model mechanical failures using an EFOR and capture resource variability. The latter is typically done using historical resource data or by simulating such data from underlying probability distributions. Reliability-based methods determine the capacity value of a generator by how it affects the system's LOLPs and LOLE. Standard reliability-based methods include the effective load-carrying capability (ELCC), equivalent conventional power (ECP), and equivalent firm power (EFP) methods, which are detailed below.

1) *Effective Load-Carrying Capability*: The ELCC of a generator is defined as the amount by which the system's loads can increase, when the generator is added to the system, while maintaining the same LOLE. The ELCC of PV is calculated by first computing the system's LOLPs without the PV as:

$$p_t = \text{Prob} \{G_t < L_t\}, \quad (1)$$

where the probability function accounts for the likelihood of generator or other failures (which are modeled using EFORs)

and can account for stochastic loads. The LOLE of the base system is then defined as:

$$\epsilon = \sum_{t \in T} p_t. \quad (2)$$

The PV plant is added to the system and a fixed load,  $\bar{L}$ , is added to each hour, giving a new LOLE:

$$\epsilon^{ELCC} = \sum_{t \in T} \text{Prob} \{G_t + V_t < L_t + \bar{L}\}, \quad (3)$$

where the probability function also accounts for the probability of real-time solar availability. The fixed load added to each hour is iteratively adjusted until the LOLE of the system with the PV and added loads is the same as that of the base system, or until:

$$\epsilon = \epsilon^{ELCC}. \quad (4)$$

The PV plant's ELCC is defined as the value of  $\bar{L}$  that achieves condition (4).

2) *Equivalent Conventional Power*: The ECP of a generator,  $g$ , is defined to be the capacity of a benchmark unit, which is assumed to have a positive EFOR, that can replace  $g$  while maintaining the same LOLE. This is an attractive measure of a renewable generator's capacity value, since it can be benchmarked against a conventional dispatchable resource. The ECP of a PV generator is calculated by first computing the LOLE of the system when the PV is added as:

$$\epsilon^{PV} = \sum_{t \in T} \text{Prob} \{G_t + V_t < L_t\}. \quad (5)$$

The LOLE of the system when only the benchmark plant (*i.e.* without the PV) is added is also computed as:

$$\epsilon^B = \sum_{t \in T} \text{Prob} \{G_t + B_t < L_t\}, \quad (6)$$

where the probability function also accounts for the likelihood of the benchmark unit failing (using an EFOR). The nameplate capacity of the benchmark unit is iteratively adjusted until the LOLE of the system with the benchmark unit is the same as that with the PV plant, or until:

$$\epsilon^{PV} = \epsilon^B. \quad (7)$$

The PV plant's ECP is defined as the nameplate capacity of the benchmark unit that achieves equality (7).

3) *Equivalent Firm Power*: A generator's EFP is computed following the same steps as the ECP, except that the benchmark plant used to compute  $\epsilon^B$  is assumed to be perfectly reliable (*i.e.* has a 0% EFOR). A generator's EFP and ELCC generally differ, since changing a system's generation mix changes the distribution of available capacity in a given hour whereas adjusting loads does not [9].

### B. Approximation Methods

While reliability-based methods are widely accepted and considered accurate capacity value estimation techniques [7], [9]–[11], they can be computationally expensive and require detailed system data. Achieving equalities (4) and (7) requires iterative LOLP calculations, which can be time-consuming.

Recent computer advances makes this less of an issue today, however [22]. Reliability-based methods also require EFORs and capacities of all existing generators in the system and loads. Moreover, due to seasonal and annual weather pattern changes, several years' data are typically needed to accurately estimate the long-run capacity value of renewables.

Because of these challenges raised by reliability-based methods, approximation techniques are typically used for capacity planning purposes [2]. These include Garver's ELCC approximation [4], the Z method [23], and capacity factor-based methods [24]. These techniques reduce the computational burden by either approximating the relationship between capacity added to the system and LOLPs or by focusing on a subset of hours during which the system faces a high risk of not serving the load. Several studies examine the accuracy of these approximation techniques in estimating the capacity value of wind and CSP. Bernow *et al.* [25] and El-Sayed [26] approximate the capacity value of wind as its average capacity factor during the highest-load hours of the year. Milligan and Parsons [24] introduce three different techniques to estimate the capacity value of wind. They approximate it as the average capacity factor during the highest-load and highest-LOLP (of the base system without added wind) hours of the year. They also approximate it as a weighted average of the capacity value during the highest-load hours of the year, using the LOLPs as weights. Madaeni *et al.* [17], [18] compare capacity factor-based and reliability-based methods applied to CSP, showing that capacity factors can provide relatively accurate approximations. Zachary and Dent [27] compare these techniques and also discuss their applicability in different settings. The approximation techniques that we consider in this analysis, which are detailed below, include capacity factor-based, Garver's, multi-state generator, and Z methods.

1) *Capacity Factor-Based Approximation*: This method approximates the capacity value of a generator as its average capacity factor over a subset of 'risky' periods. Hours with high loads or LOLPs are typically used. We focus on the weighted capacity factor method that Milligan and Parsons [24] apply to wind. This method approximates the capacity value by first determining a subset of hours,  $T'$ , with the highest loads, over which the capacity factor is averaged. The weights used in each hour are then computed as:

$$w_t = \frac{p_t}{\sum_{\tau \in T'} p_\tau}, \quad (8)$$

where the  $p_t$ 's are the LOLPs of the base system, without added PV, and are calculated using (1). The capacity value of the PV plant is approximated as:

$$\frac{\sum_{t \in T} w_t \cdot V_t}{\bar{V}}. \quad (9)$$

2) *Garver's Approximation Method*: Garver [4] proposes an ELCC approximation, which uses the exponential risk function:

$$\epsilon \approx \sum_{t \in T} B \cdot \exp\left(-\frac{\bar{G} - L_t}{m}\right), \quad (10)$$

to relate the system's LOLE to its excess generation capacity. The parameter,  $m$ , is called the system characteristic and represents the amount of additional load, in MW, that gives an LOLE that is  $\epsilon$  times greater than before. The values of  $B$  and  $m$  are typically estimated by conducting multiple LOLE calculations using (1) and (2) and fitting their values to the data. The PV plant is added to the system and a fixed load is added to each hour, giving the new approximated LOLE:

$$\epsilon^{ELCC} \approx \sum_{t \in T} B \cdot \exp\left(-\frac{\bar{G} + V_t - L_t - \bar{L}}{m}\right). \quad (11)$$

The ELCC of the plant is approximated as the value of  $\bar{L}$  that equates these two LOLEs, or such that:

$$\sum_{t \in T} B \cdot \exp\left(-\frac{\bar{G} - L_t}{m}\right) = \sum_{t \in T} B \cdot \exp\left(-\frac{\bar{G} + V_t - L_t - \bar{L}}{m}\right). \quad (12)$$

Solving for  $\bar{L}$  yields:

$$\bar{L} = m \cdot \log\left(\frac{\sum_{t \in T} \exp\left(\frac{L_t}{m}\right)}{\sum_{t \in T} \exp\left(\frac{L_t - V_t}{m}\right)}\right). \quad (13)$$

3) *ELCC Approximation for Multi-State Generators*: This method generalizes Garver's approximation to multi-state generators [19]. The focus is on approximating the ELCC of wind, which is multi-state since different weather conditions result in different real-time wind availability states. Thus, the method should be appropriate for other renewables with weather-related resource constraints. However, it can also be applied to conventional generators that experience different outage states (e.g. operating at reduced capacity due to an outage).

The method assumes that the probabilities with which the generator being analyzed can be in the different possible states is time-invariant. It further relies on the same exponential risk function (10) used by Garver to approximate LOLEs based on the system's excess generating capacity. D'Annunzio and Santoso's [19] derivation gives the closed-form value:

$$-\frac{1}{m} \log\left[\sum_{\omega \in \Omega} \pi_\omega \cdot \exp(m \cdot (V_\omega - \bar{V}))\right], \quad (14)$$

for the approximated ELCC of a PV plant.

4) *Z Method*: The Z method focuses on the difference between available generating capacity and load:

$$S_t = G_t - L_t, \quad (15)$$

during peak hours. Dragoon and Dvortsov [23] argue that in a large power system with many generators, the central limit theorem implies that  $S_t$  should have a Gaussian distribution. Thus, they argue that the ratio between the mean and standard deviation of  $S_t$  (computed over peak-load hours of the year):

$$Z = -\frac{\mu_S}{\sigma_S}, \quad (16)$$

is an indicator of a system's resource adequacy. They further argue that although adding capacity or load to the system can

change the mean and variance of  $S_t$ , its distribution remains Gaussian. Thus, they estimate the ELCC of a generator as the load that must be added in each hour to maintain the same  $Z$  value when the generator is added to the system. Adding a fixed load,  $\bar{L}$ , in each hour and a PV plant changes the mean and standard deviation of  $S_t$  to  $\mu_S + \mu_{PV} - \bar{L}$  and  $\sqrt{\sigma_S^2 + \sigma_{PV}^2}$ , respectively. Thus, maintaining the same  $Z$ -statistic after the load and PV are added requires:

$$-\frac{\mu_S}{\sigma_S} = \frac{\bar{L} - \mu_S - \mu_{PV}}{\sqrt{\sigma_S^2 + \sigma_{PV}^2}}. \quad (17)$$

Solving for  $\bar{L}$  gives:

$$\bar{L} = \mu_{PV} + Z \left( \sqrt{\sigma_S^2 + \sigma_{PV}^2} - \sigma_S \right), \quad (18)$$

which is typically simplified to:

$$\bar{L} \approx \mu_{PV} + Z \frac{\sigma_{PV}^2}{2\sigma_S}, \quad (19)$$

using a first-order Taylor approximation in  $\sigma_{PV}^2$  of the radical term in (18).

The  $Z$  method relies critically on the assumption that the distribution of  $S_t$  remains Gaussian when new generation and loads are added. With conventional dispatchable generators only, this is a relatively innocuous assumption since generator failures are typically assumed to occur independently of one another and the central limit theorem applies. With high penetrations of renewables this may not hold true, however, since energy available from two plants may be correlated.

### III. CASE STUDY AND DATA

We estimate the capacity value of PV at the 14 sites in the western United States listed in Table I. As discussed in section III-B, we hold the underlying power system characteristics (such as load patterns) fixed at all locations, allowing the effect of differences in solar availability patterns on the capacity value of PV to be directly ascertained, without differences in the power system confounding the results. These sites are chosen to represent a mix of locations that either have relatively good solar resource or are within urban areas. While they may have less solar resource available, PV in urban areas can be attractive since the plant is co-located with load. Moreover, rooftop PV can be more easily deployed in populated areas. Our analysis considers small 100 MW PV plants at each location. Thus, our capacity value estimates are for marginal PV installations, and do not account for the diminishing marginal capacity value that occurs with higher PV penetrations. Moreover, the capacity values at the locations are computed in isolation. Thus, our estimates are non-additive, since they do not account for spatial correlation of solar availability between locations.

#### A. Photovoltaic Model

We model PV generation using version 2011.6.30 of the National Renewable Energy Laboratory's Solar Advisor Model (SAM) [28]. SAM takes weather data, including solar irradiation and temperature, as inputs and simulates hourly net ac

TABLE I  
LOCATION OF PV PLANTS STUDIED

Site	Coordinates	Characteristic
Barstow, CA	35.15° N, 117.35° W	High Solar
Congress, AZ	34.15° N, 113.15° W	High Solar
Yucca Flat, NV	37.25° N, 116.15° W	High Solar
Hanover, NM	33.05° N, 107.75° W	High Solar
Cheyenne, WY	41.35° N, 104.95° W	Urban Area
Salt Lake City, UT	41.05° N, 112.05° W	Urban Area
Boise, ID	43.85° N, 116.25° W	Urban Area
Los Angeles, CA	34.45° N, 118.45° W	Urban Area
San Francisco, CA	37.85° N, 122.45° W	Urban Area
Seattle, WA	47.75° N, 122.45° W	Urban Area
Denver, CO	39.95° N, 104.85° W	Urban Area
Albuquerque, NM	35.25° N, 106.65° W	Urban Area
Phoenix, AZ	33.45° N, 111.95° W	Urban Area
Las Vegas, NV	36.25° N, 115.15° W	Urban Area

electrical output of a PV plant. It accounts for power electronic efficiency losses and other parasitic loads. Each PV plant's hourly net ac outputs are used as inputs for the capacity valuation methods discussed in section II. In all of our analyses we assume a PV plant with a nameplate capacity of 100 MW-DC. This corresponds to 83.4 MW-AC under standard test conditions (STC) of 1000 W/m<sup>2</sup> of solar irradiation and 25° C cell temperature [28]. This ac rating is used to normalize the capacity values estimated. The 83.4 MW-AC under STC is not necessarily the maximum ac capacity of the plant. Indeed, there can be conditions (*e.g.* high solar irradiation or low cell temperature) under which the PV plant generates more than 83.4 MW, which could yield a capacity value greater than 100%.

SAM includes four PV performance models [28], and our analysis is based on the California Energy Commission model. Inverter characteristics are based on the Sandia Inverter Performance model. These inverters have a non-linear behavior, making them significantly more efficient at high power outputs. We assume a Satcon Technology Corporation PVS-250 inverter is used, however the results are extremely insensitive to this assumption. We compare the modeled output of a fixed-axis PV plant located in Barstow, CA using the Satcon and three additional inverters (Eaton SM1003, Kacon New Energy Blue Plant XP 100U, and Xantrex Technologies GT 100). The maximum change in the generation profile is less than 0.6%.

Our base case assumes fixed-axis PV panels that are oriented southward with an azimuth angle<sup>1</sup> of 0° and a tilt angle<sup>2</sup> equal to the site's latitude. Changing the orientation or tilt angle can affect capacity value, since it affects total energy yield and favors either morning or afternoon generation. Section V presents a sensitivity analysis of the effect of including single- and double-axis sun-tracking systems on the capacity value of PV.

#### B. Data Sources

Our analysis uses eight years of hourly historical conventional generator, load, and weather data from 1998 to 2005.

<sup>1</sup>Azimuth angle measures east to west orientation of a PV panel. A 0° azimuth angle corresponds to southward orientation, while 90° and -90° correspond to a westward and eastward orientation, respectively.

<sup>2</sup>Tilt angle is defined as the angle between the horizontal and the inclination of the PV array.

Since all of the locations are within the Western Electricity Coordinating Council (WECC) region, this analysis uses the entire WECC footprint to determine system loads and LOLPs. This assumes a ‘copperplated’ system with sufficient transmission capacity to move PV generation wherever it is needed in the system to serve the load. If binding transmission constraints limit the amount of PV generation that can serve the load during high-LOLP hours, capacity values may be lower than the values reported here. Utilities and system planners often use smaller footprints in their capacity planning, since they are primarily interested in ensuring reliability within the limited territory that they serve. Thus, the capacity values reported here may be different from the results of such an analysis. This is because PV output may be more or less coincident with the ‘local’ load of a more limited system than it is with the WECC-wide load [15], [29].

We model generator outages using a simple two-state (on-line/offline) model. LOLPs are estimated by computing the system’s capacity outage table, which assumes that generator outages follow serially and jointly independent Bernoulli distributions [5]. Data requirements and sources used for our analysis are detailed below.

1) *Conventional Generators*: Each generator’s rated capacity is obtained from Form 860 data filed with the United States Department of Energy’s Energy Information Administration (EIA). The EIA data specify a winter and summer capacity, which capture the effect of ambient temperature on the maximum operating point of thermal generators. The WECC had between 1,016 and 1,622 generating units and 123 GW and 163 GW of generating capacity during the years that we study, reflecting load growth during this period.

We estimate EFORs of the existing generator fleet using the North American Electric Reliability Corporation’s Generating Availability Data System (GADS). The GADS specifies historical annual average generator EFORs based on generating capacity and technology. We combine these with EIA Form 860 data, which specify generator prime mover and generating fuel, to estimate EFORs. The EFORs used range between 2% and 17% and have a capacity-weighted average of 7% for the entire WECC.

We use a natural gas-fired combustion turbine as the benchmark unit, against which PV is compared, in the ECP method. This is because such generators are often built for peak-capacity purposes. We assume a 7% EFOR for the combustion turbine, based on values reported in the GADS. The ECP of a PV plant is sensitive to this assumption, since different generation technologies against which it can be benchmarked have different EFORs.

2) *Load*: Hourly historical WECC load data for each year are obtained from Form 714 filings with the Federal Energy Regulatory Commission (FERC). The FERC data include load reports for nearly all of the load-serving entities and utilities in the WECC, although some smaller municipalities and cooperatives are not reflected in the data. We assume loads are fixed and deterministic based on these data, which have annual peaks ranging between 107 GW and 124 GW. Since the system loads increased over the study period and capacity expansion can lead or lag such growth, we adjust the hourly

load profiles in each year individually so that the LOLPs of the base system in each year sum to 2.4. This corresponds to the standard planning target of one outage-day every 10 years [30]. This load adjustment is done by scaling all of the hourly loads by a fixed percentage, ranging between 0.1% and 5% in the different years. Fig. 1 shows hourly loads during the highest-load, a winter, and the lowest-load weeks of 2003. These loads correspond to the weeks beginning 20 July, 12 January, and 11 May, respectively, and illustrate typical WECC summer, winter, and spring load patterns.

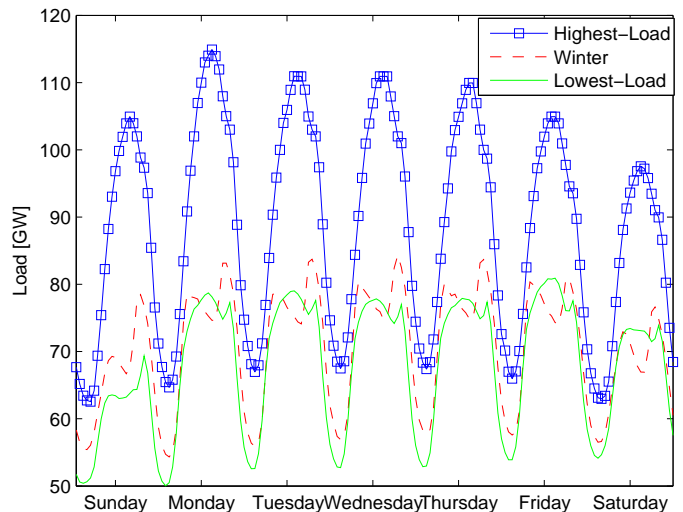


Fig. 1. Hourly loads during the highest-load, a winter, and the lowest-load weeks of 2003.

3) *Weather*: SAM requires detailed weather data, including solar irradiation, temperature, and wind speed. These data are obtained from the National Solar Radiation Data Base [31], which accounts for cloud cover and other factors.

#### IV. CAPACITY VALUE OF PHOTOVOLTAIC SOLAR

##### A. Reliability-Based Methods

Table II summarizes average annual capacity values over the eight years studied using the ECP and ELCC methods. The table shows that ELCCs are less than ECPs. This is because PV is benchmarked against a generator with a positive EFOR (assumed to be 7%) in the ECP method. With ELCC, however, PV is compared to a constant load, which is akin to a fully-reliable generator with a 0% EFOR. PV has a lower capacity value when compared to a fully-reliable generator, as illustrated in Table II.

Depending on location, the ECP of PV can range from 56% to 75% and ELCC can range from 52% to 70%, which is broadly consistent with other PV analyses [15], [29]. Hoff *et al.* [15] approximate the ELCC of fixed-axis PV with a southwesterly orientation and a 30° tilt angle in the year 2002 using Garver’s approximation method. They estimate the ELCC of 100 MW of PV to be about 70% and 30% in the Nevada Power and Portland General Electric systems. While their Nevada result is within our range of ELCCs, their estimated capacity value for Portland, OR is significantly lower. This is, in large part, due to our use of

TABLE II  
AVERAGE ANNUAL CAPACITY VALUE OF PV

Site	ECP	ELCC
Barstow, CA	64.2	59.7
Congress, AZ	75.1	69.7
Yucca Flat, NV	61.0	56.6
Hanover, NM	61.0	56.7
Cheyenne, WY	55.8	51.8
Salt Lake City, UT	65.7	61.0
Boise, ID	71.1	66.0
Los Angeles, CA	56.0	52.0
San Francisco, CA	60.1	55.8
Seattle, WA	62.0	57.6
Denver, CO	64.6	60.0
Albuquerque, NM	72.6	67.4
Phoenix, AZ	69.4	64.4
Las Vegas, NV	64.6	60.0

the entire WECC footprint in our analysis, whereas Hoff *et al.* use the Portland General Electric system only. While the summer solar resource in Portland, OR correlates well with the WECC-wide load, Portland General Electric was a winter-peaking system in 2002. Thus PV has a much more limited contribution to system reliability when this limited footprint is used. Nevada Power, by contrast, is a summer-peaking system with large commercial air conditioning demands. Thus, the Nevada Power load is more strongly correlated with WECC-wide loads and the output of PV plants in Nevada. Perez *et al.* [32] study the relationship between the capacity value of PV and the ratio of the system's summer and winter peak load. By examining systems with different ratios they are able to show the sensitivity of the capacity value to this ratio.

Because our analysis uses the same load pattern for all locations, the different capacity values depend solely on regional variations in solar resource. For instance, PV located in Congress, AZ, which receives relatively high solar irradiation, has a 75% average annual ECP. PV located in Los Angeles, CA only has a 56% ECP. This difference is due to lower correlation between WECC-wide loads and PV generation in Los Angeles compared to Congress. To illustrate this, Fig. 2 shows the output of PV in Congress and Los Angeles on 20 July, 2005. This is the day with the highest WECC-wide load of 2005. As the figure shows, PV generation in Congress is more coincident with the load than that in Los Angeles. In hour 14, when the load reaches its annual peak, the PV in Congress produces 66 MW as opposed to only 16 MW in Los Angeles. Since generation during peak-load hours has a direct impact on capacity value, the PV in Los Angeles has a lower capacity value than that in Congress. It is important to stress that any correlation between local loads and PV generation in Los Angeles and Congress are not captured in our analysis, since we use a WECC-wide footprint in our analysis.

Table II also shows that there are locations, such as Boise, ID and Seattle, WA, with high capacity values despite having relatively low solar resource. This is because peaks in solar irradiation and PV generation at these locations are coincident with peaks in the WECC load. Although total generation at such locations is low compared to other parts of the WECC, the contribution toward reliably serving the load is high.

The values shown in Table II are annual averages. We find

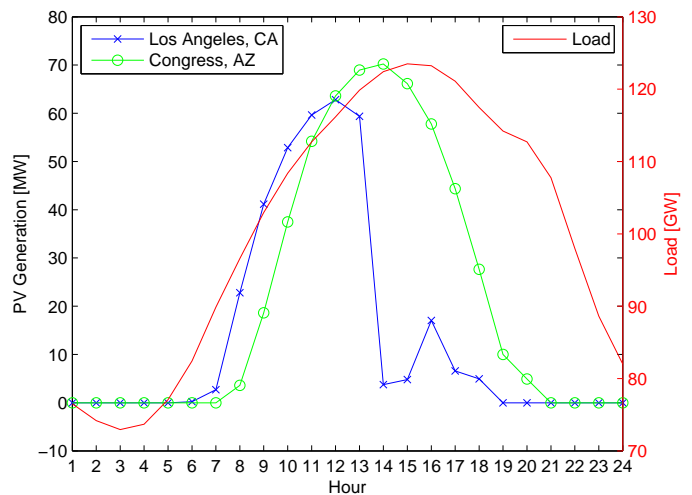


Fig. 2. Hourly loads and output of a fixed-axis PV plant located in Los Angeles, CA and Congress, AZ on 20 July, 2005.

significant interannual variation in capacity values between the years studied, however. For instance, the ECP of PV in Congress, AZ ranges from 48% in 1999 to 85% in 2002. This is because solar availability patterns vary considerably from one year to another, resulting in solar output that is less coincident with system loads in some years. Fig. 3 demonstrates this by showing hourly loads and PV output in Congress on 12 July, 1999 and 10 July, 2002. These are days on which the load reaches its annual peak. As the figure shows, PV output is significantly less coincident with load on the day in 1999. When the load reaches its peak in hours 16 and 17 in 1999, the PV is producing an average of 10 MW. Conversely, PV generation is 68 MW in hour 14 when the load peaks in 2002. This interannual variability indicates that several years of data are necessary for an accurate and robust long-term estimate of capacity value, as with wind and CSP [7], [17], [22]. Moreover, using multiple years of data to arrive at a single long-term capacity value, as opposed to averaging single-year capacity values as we do, may provide more robust estimates.

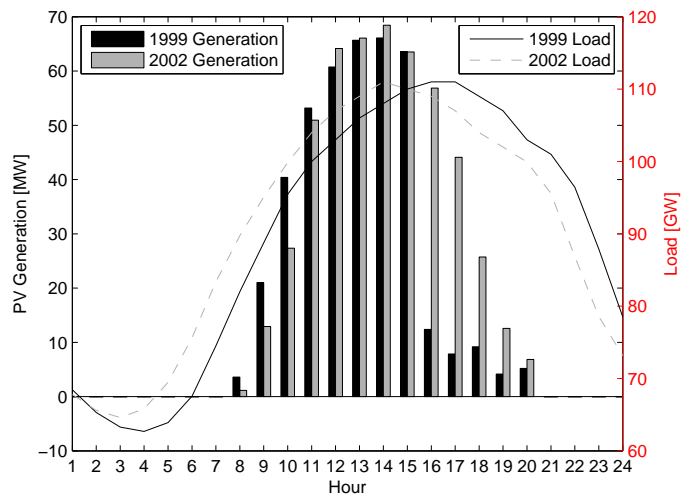


Fig. 3. Hourly loads and dispatch of a fixed-axis PV plant located in Congress, AZ on 12 July, 1999 and 10 July, 2002.

## B. Approximation Methods

Table III summarizes average annual capacity values of PV at each location using the approximation methods detailed in section II-B. Since these methods are intended to approximate ELCC, the table also provides ELCCs for purposes of comparison. The capacity factor-based approximation reported in the table is the LOLP-weighted method, using the 10 highest-load hours of the year. Madaeni *et al.* [17], [18] show that when applied to CSP, the LOLP-weighted method provides more accurate approximations than using the highest-load or highest-LOLP methods. This is because the weighted method places proportionally higher weight on generation during hours with relatively high LOLPs. They further show that using the 10 highest-load hours provides the best approximation, and we find the same results for PV. Specifically, we compare capacity factor-based approximations using the 100 and 876 (10%) highest-load hours, and find 10 hours to provide the closest approximation. This is because the capacity value of (CSP and PV) solar is highly sensitive to the most critical hours of the year, due to strong correlation between loads and generation. Adding more hours to the calculation reduces the approximated capacity value, biasing the result. Conversely, Milligan and Parsons [24] show that a capacity factor-based approximation of wind requires the 10% highest-load hours to be used. Wind requires more periods to be included due to the weaker correlation between loads and generation. If too few hours are considered, the approximation is biased downward.

The Garver and multi-state generator approximation methods require estimating the parameters  $m$  and  $B$ . The multi-state generator method further requires a probability distribution representing the possible states in which the PV plant can operate. We approximate a different value for  $m$  and  $B$  in each year by estimating the LOLE of the system with different load peaks. This is done by adding a constant load in each hour, equal to 5% and 10% of the annual peak load, and estimating the LOLE using (2). We also estimate LOLEs by subtracting a constant load equal to 5% and 10% of the annual peak. This gives five LOLEs corresponding to different load patterns (including the LOLE of the base system with unadjusted loads). Values for  $m$  and  $B$  are found by fitting (10) to the data using ordinary least squares. This yields values for  $m$  ranging between  $6.9 \times 10^{-6}$  and  $8.7 \times 10^{-6}$  in the different years.

We use four different probability distributions in the multi-state generator method. The first uses the empirical distribution of hourly PV output in each year. That is, we assume the PV plant can operate in 8760 different states, corresponding to the modeled output of the plant in each hour of the year, each having equal probability. Table III shows that representing PV generation in this manner significantly underestimates the ELCC, since a high probability is placed on 0 output (which occurs during night hours). To overcome this, we use three coarser representations of the probability distribution in which the empirical data are aggregated into 10, 20, or 33 MW ‘blocks.’ This is done by binning the modeled generation. For instance, with 20 MW blocks the bins correspond to outputs between 0 and 20 MW, 20 and 40 MW, 40 and 60 MW, *etc.*

Each bin represents one possible state, with the probability determined by the number of observations falling within the bin. The output when the generator is in each state is given by the midpoint of the bin. Thus, with the above example with 20 MW blocks, the output of the PV plant in each state is 10 MW, 30 MW, 50 MW, *etc.* Table III shows that these coarser representations of the probability distribution yield capacity value approximations approaching the ELCC. This is because the coarser bins reduce the effect of low generation, which occurs during night and shoulder hours, biasing the approximation downward.

The Z method approximates the capacity value based on the mean and standard deviation of surplus capacity in the base system during peak-load hours and PV generation. We compute different values for  $\mu_S$  and  $\sigma_S$  in each year based on the 10 highest-load hours. This gives values between 4600 MW and 7400 MW for  $\mu_S$  and between 2500 MW and 4800 MW for  $\sigma_S$ . We estimate different values for the mean and standard deviation of PV generation in each year based on simulated hourly generation. This gives means ranging between 25.4 MW and 66.7 MW and standard deviations between 4.4 MW and 28.7 MW.

Table III shows that while some methods provide relatively good approximations of a more detailed ELCC, others are significantly less accurate. To measure the relative accuracy of the different approximation techniques, we use a root-mean-square error (RMSE) metric to compare each method to the ELCC. This RMSE is defined as:

$$\sqrt{\frac{1}{|\Lambda|} \sum_{\lambda \in \Lambda} (c_{\lambda}^{ELCC} - c_{\lambda}^a)^2}, \quad (20)$$

and is based on the difference between the annual average capacity value estimated using the ELCC and approximation method  $a$ . These differences are averaged over the locations modeled. Table IV summarizes the RMSEs for the different approximation techniques, showing that the capacity factor-based approximation provides the best overall approximation to the ELCC. Moreover, it shows that if applied properly (*i.e.* an appropriate probability distribution is used to represent the possible operating states of PV in the multi-state method), all of the approximation methods are comparable to each other in accuracy.

TABLE IV  
AVERAGE ROOT-MEAN-SQUARE ERROR OF DIFFERENT APPROXIMATION TECHNIQUES

Method	RMSE
Capacity Factor	4.4
Garver	7.4
Multi-State Generator	
Empirical	37.9
10 MW	28.7
20 MW	19.5
33 MW	7.7
Z	8.3

## V. SENSITIVITY TO SUN-TRACKING SYSTEMS

Our analysis thus far assumes fixed-axis PV panels. Single- and double-axis sun-tracking systems, which adjust the real-



TABLE III  
AVERAGE ANNUAL CAPACITY VALUE OF PV

Site	ELCC	Capacity Factor	Garver	Multi-State Generator			Z	
				Empirical	10 MW	20 MW		33 MW
Barstow, CA	59.7	60.4	58.3	25.4	34.8	43.9	57.6	46.8
Congress, AZ	69.7	70.4	62.7	24.6	33.9	43.6	56.5	61.8
Yucca Flat, NV	56.6	57.9	55.5	25.2	34.6	44.0	57.2	44.5
Hanover, NM	56.7	57.3	50.1	24.3	33.6	43.1	56.2	48.4
Cheyenne, WY	51.8	57.3	55.8	22.1	31.5	40.9	54.7	46.8
Salt Lake City, UT	61.0	67.7	60.9	24.7	34.0	43.2	57.1	52.4
Boise, ID	66.0	72.6	60.1	23.3	32.6	42.5	54.9	56.6
Los Angeles, CA	52.0	56.8	54.6	24.0	33.3	42.9	55.7	49.5
San Francisco, CA	55.8	61.2	45.0	22.0	31.3	40.8	54.5	53.4
Seattle, WA	57.6	66.2	54.7	20.9	30.1	40.0	53.0	62.2
Denver, CO	60.0	61.6	60.6	20.6	30.0	39.7	53.1	66.6
Albuquerque, NM	67.4	69.8	51.8	23.1	32.4	41.3	55.7	52.6
Phoenix, AZ	64.4	65.9	51.9	19.9	29.2	38.8	52.3	58.3
Las Vegas, NV	60.0	62.8	50.7	14.9	24.2	33.9	48.3	60.2

time orientation of the panel to track the location of the sun, can be added to increase generation. A single-axis tracking system is typically untilted, but rotates the panel about the azimuth angle to follow daily movement of the sun. A double-axis tracking system rotates the panel about both the azimuth and tilt angle, allowing the panel to track the daily and seasonal movement of the sun.

Table V summarizes the ECP and ELCC of PV plants with single- or double-axis sun-tracking systems. Comparing to the values reported in Table II shows, as expected, that sun-tracking systems increase capacity value, with double-axis systems having the greatest effect. Whereas fixed-axis PV have ECPs ranging between 56% and 75%, a double-axis tracking system increases the ECP to between 71% and 93%.

TABLE V  
AVERAGE ANNUAL CAPACITY VALUE OF PV WITH SUN-TRACKING SYSTEM

Site	Single-Axis		Double-Axis	
	ECP	ELCC	ECP	ELCC
Barstow, CA	78.3	72.7	79.4	73.7
Congress, AZ	82.7	76.8	85.7	79.5
Yucca Flat, NV	74.2	68.9	76.1	70.7
Hanover, NM	70.3	65.3	71.2	66.2
Cheyenne, WY	77.9	72.4	80.5	74.8
Salt Lake City, UT	84.7	78.7	88.6	82.2
Boise, ID	87.4	81.2	92.2	85.6
Los Angeles, CA	83.4	77.4	85.0	78.9
San Francisco, CA	83.0	77.1	84.5	78.4
Seattle, WA	87.2	80.9	92.7	86.1
Denver, CO	75.1	69.8	77.9	72.3
Albuquerque, NM	84.6	78.5	86.5	80.3
Phoenix, AZ	77.1	71.6	78.2	72.6
Las Vegas, NV	82.6	76.7	84.6	78.5

## VI. CONCLUSIONS

This paper compares several approaches for estimating the capacity value of PV. It applies these methods at a variety of locations within the WECC between the years 1998 and 2005, while assuming the load is fixed to evaluate the variation in performance based on the solar resource. This is done by simulating hourly PV generation and using it as an input to reliability-based methods and approximation techniques. While ECP and ELCC are well recognized and widely used, we find that some approximation techniques can yield similar

results. Our results show that PV, on average, can have ELCCs between 52% and 93% depending on the location and sun-tracking capability of the plant. As with other renewable resources, we find high interannual variation of about 16%, indicating that multiple years of data are required for a robust estimation of capacity value. Out of the approximation techniques that we study, we find the capacity factor-based method to be the most accurate technique on the basis of an RMSE metric. This is important, given the use of approximation techniques by system operators and utilities in their long-term capacity planning [2]. Overall, our analysis indicates that these approximation techniques provide relatively robust estimates of PV capacity value for use in other systems. Although we estimate capacity values by modeling the entire WECC, these techniques could be applied to the more limited footprints often used by system planners and utilities.

The WECC-wide results presented here may differ from analysis of smaller regions, depending on the extent to which solar resource is coincident with the ‘local’ load. For instance, the northwestern United States is typically a winter-peaking system, and PV generation in these areas is typically less coincident with the ‘local’ load than with the WECC-wide load. Thus, PV in the Northwest may have lower capacity values than our estimates suggest if this more limited footprint is used. By modeling the entire WECC system we also assume that the system has sufficient transmission capacity to deliver power wherever it is needed. If binding transmission constraints prevent this, actual ECPs could be lower than our estimates [2]. Additional analysis is needed to consider both the local coincidence of PV with demand and the ability of transmission to share capacity across larger regions of an interconnected system.

## ACKNOWLEDGMENT

The authors would like to thank C. Dent, V. Banunarayanan, M. Milligan, R. Newmark, and A. Sorooshian for helpful discussions and suggestions.

## REFERENCES

- [1] G. R. Pudaruth and F. Li, “Capacity credit evaluation: A literature review,” in *Third International Conference on Electric Utility Deregulation and Restructuring and Power Technologies*. Nanjing, China: Institute of Electrical and Electronics Engineers, 6-9 April 2008, pp. 2719–2724.



- [2] *Methods to Model and Calculate Capacity Contributions of Variable Generation for Resource Adequacy Planning*, North American Electric Reliability Corporation, Princeton, New Jersey, March 2011.
- [3] C. F. DeSieno and L. L. Stine, "A probability method for determining the reliability of electric power systems," *IEEE Transactions on Reliability*, vol. R-14, pp. 30–35, March 1965.
- [4] L. L. Garver, "Effective load carrying capability of generating units," *IEEE Transactions on Power Apparatus and Systems*, vol. PAS-85, pp. 910–919, August 1966.
- [5] R. Billinton and R. N. Allan, *Reliability Evaluation of Power Systems*. Boston: Pitman Advanced Publishing Program, 1984.
- [6] M. R. Milligan, "Measuring wind plant capacity value," National Renewable Energy Laboratory, Tech. Rep. NREL/TP-441-20493, 1996.
- [7] M. R. Milligan and B. Parsons, "Comparison and case study of capacity credit algorithms for intermittent generators," National Renewable Energy Laboratory, Tech. Rep. NREL/CP-440-22591, March 1997.
- [8] M. R. Milligan and T. Factor, "Optimizing the geographic distribution of wind plants in iowa for maximum economic benefit and reliability," *Wind Engineering*, vol. 24, pp. 271–290, July 2000.
- [9] C. Ensslin, M. R. Milligan, H. Holttinen, M. O'Malley, and A. Keane, "Current methods to calculate capacity credit of wind power, iea collaboration," in *2008 IEEE Power and Energy Society General Meeting*. Pittsburgh, PA, USA: Institute of Electrical and Electronics Engineers, 20–24 July 2008.
- [10] M. Amelin, "Comparison of capacity credit calculation methods for conventional power plants and wind power," *IEEE Transactions on Power Systems*, vol. 24, pp. 685–691, May 2009.
- [11] A. Keane, M. R. Milligan, C. J. Dent, B. Hasche, C. D'Annunzio, K. Dragoon, H. Holttinen, N. Samaan, L. Söder, and M. O'Malley, "Capacity value of wind power," *IEEE Transactions on Power Systems*, vol. 26, pp. 564–572, May 2011.
- [12] R. Perez, R. Seals, and R. Stewart, "Assessing the load matching capability of photovoltaics for us utilities based upon satellite-derived insolation data," in *Conference Record of the Twenty Third IEEE Photovoltaic Specialists Conference*. Louisville, KY, USA: Institute of Electrical and Electronics Engineers, 10–14 May 1993, pp. 1146–1151.
- [13] R. Perez, R. Margolis, M. Kmiecik, M. Schwab, and M. Perez, "Update: Effective load-carrying capability of photovoltaics in the United States," National Renewable Energy Laboratory, Tech. Rep. NREL/CP-620-40068, June 2006.
- [14] R. Perez, M. Kmiecik, J. Schlemmer, L. Root, K. Moore, and P. Stackhouse, "Evaluation of pv generation capacity credit forecast on day-ahead utility markets," in *Solar 2007, Including Proceedings from the 36th ASES Annual Conference, 32nd National Passive Solar Conference, and 2nd Renewable Energy Policy and Marketing Conference "Sustainable Energy Puts America to Work"*, R. Campbell-Howe, Ed. American Solar Energy Society, September 2007, pp. 75–80.
- [15] T. Hoff, R. Perez, J. P. Ross, and M. Taylor, "Photovoltaic capacity valuation methods," Solar Electric Power Association, SEPA Report 02-08, May 2008.
- [16] S. Pelland and I. Abboud, "Comparing photovoltaic capacity value metrics: A case study for the city of Toronto," *Progress in Photovoltaics: Research and Applications*, vol. 16, pp. 715–724, December 2008.
- [17] S. H. Madaeni, R. Sioshansi, and P. Denholm, "Estimating the capacity value of concentrating solar power plants: A case study of the southwestern United States," *IEEE Transactions on Power Systems*, vol. 27, pp. 1116–1124, May 2012.
- [18] —, "Estimating the capacity value of concentrating solar power plants with thermal energy storage: A case study of the southwestern United States," *IEEE Transactions on Power Systems*, 2012, forthcoming.
- [19] C. D'Annunzio and S. Santoso, "Noniterative method to approximate the effective load carrying capability of a wind plant," *IEEE Transactions on Energy Conversion*, vol. 23, pp. 544–550, June 2008.
- [20] M. R. Milligan and K. Porter, "Determining the capacity value of wind: An updated survey of methods and implementation," National Renewable Energy Laboratory, Tech. Rep. NREL/CP-500-43433, June 2008.
- [21] L. Söder and M. Amelin, "A review of different methodologies used for calculation of wind power capacity credit," in *2008 IEEE Power and Energy Society General Meeting*. Pittsburgh, PA, USA: Institute of Electrical and Electronics Engineers, 20–24 July 2008.
- [22] B. Hasche, A. Keane, and M. O'Malley, "Capacity value of wind power, calculation, and data requirements: the irish power system case," *IEEE Transactions on Power Systems*, vol. 26, pp. 420–430, February 2011.
- [23] K. Dragoon and V. Dvortsov, "Z-method for power system resource adequacy applications," *IEEE Transactions on Power Systems*, vol. 21, pp. 982–988, May 2006.
- [24] M. R. Milligan and B. Parsons, "Comparison and case study of capacity credit algorithms for wind power plants," *Wind Engineering*, vol. 23, pp. 159–166, May 1999.
- [25] S. Bernow, B. Biewald, J. Hall, and D. Singh, "Modelling renewable electric resources: A case study of wind," Oak Ridge National Laboratory, Tech. Rep. ORNL/Sub-93-03370, July 1994.
- [26] M. A. H. El-Sayed, "Substitution potential of wind energy in egypt," *Energy Policy*, vol. 30, pp. 681–687, June 2002.
- [27] S. Zachary and C. J. Dent, "Probability theory of capacity value of additional generation," *Journal of Risk and Reliability*, vol. 226, pp. 33–43, February 2012.
- [28] P. Gilman, N. Blair, M. Mehos, C. B. Christensen, and S. Janzou, "Solar advisor model user guide for version 2.0," National Renewable Energy Laboratory, Tech. Rep. NREL/TP-670-43704, August 2008.
- [29] *An Effective Load Carrying Capacity Analysis for Estimating the Capacity Value of Solar Generation Resources on the Public Service Company of Colorado System*, Xcel Energy Services, Inc., February 2009.
- [30] E. P. Kahn, "Effective load carrying capability of wind generation: Initial results with public data," *The Electricity Journal*, vol. 17, pp. 85–95, December 2004.
- [31] S. Wilcox, "National solar radiation database 1991-2005 update: User's manual," National Renewable Energy Laboratory, Tech. Rep. NREL/TP-581-41364, April 2007.
- [32] R. Perez, M. Taylor, T. Hoff, and J. P. Ross, "Reaching consensus in the definition of photovoltaics capacity credit in the usa: A practical application of satellite-derived solar resource data," *IEEE Journal of Selected Topics in Applied Earth Observations and Remote Sensing*, vol. 1, pp. 28–33, March 2008.



**Seyed Hossein Madaeni** (S'11) holds the B.S. and M.S. degrees in electrical engineering from the University of Tehran and the Ph.D. in industrial and systems engineering from The Ohio State University.

He is a Senior Energy Supply Analyst in the Short Term Electric Supply Department at Pacific Gas and Electric Company, San Francisco, CA. His research focuses on electricity market design and mechanisms, renewable energy analysis, and power system operations.



**Ramteen Sioshansi** (M'11–SM'12) holds the B.A. degree in economics and applied mathematics and the M.S. and Ph.D. degrees in industrial engineering and operations research from the University of California, Berkeley, and an M.Sc. in econometrics and mathematical economics from The London School of Economics and Political Science.

He is an assistant professor in the Integrated Systems Engineering Department at The Ohio State University, Columbus, OH. His research focuses on renewable and sustainable energy system analysis and the design of restructured competitive electricity markets.



**Paul Denholm** (M'11–SM'12) holds the B.S. degree in physics from James Madison University, the M.S. in instrumentation physics from the University of Utah, and the Ph.D. in land resources/energy analysis and policy from the University of Wisconsin-Madison.

He is a senior analyst in the Strategic Energy Analysis Center at the National Renewable Energy Laboratory, Golden, CO. His research interests are in the effects of large-scale renewable energy deployment in electric power systems, and renewable energy enabling technologies such as energy storage and long distance transmission.